



PERGAMON

Organic Geochemistry 31 (2000) 919–930

www.elsevier.nl/locate/orggeochem

**Organic
Geochemistry**

Marine and terrestrial biomarker records for the last 35,000 years at ODP site 658C off NW Africa

Meixun Zhao ^{a,*}, Geoffrey Eglinton ^b, Simon K. Haslett ^c, Richard W. Jordan ^d,
Michael Sarnthein ^e, Zhaohui Zhang ^a

^aDepartment of Earth Sciences, Dartmouth College, Hanover, NH 03755, USA

^bBiogeochemistry Centre, Department of Geology, University of Bristol, Bristol BS8 1RJ, UK

^cQuaternary Research Unit, Faculty of Applied Science, Bath Spa University College, Bath BA2 9BN, UK

^dDepartment of Earth & Environmental Sciences, Faculty of Science, Yamagata University, 990 Japan

^eGeologisch-Palaeontologisches Institut, Universitaet Kiel, D-24098 Kiel, Germany

Received 4 February 1999; accepted 27 February 2000
(returned to author for revision 11 June 1999)

Abstract

Several high-resolution proxy environmental records have been obtained for the last 35 kyr from ODP Hole 658C, a well-studied site ca. 200 km off Cap Blanc, NW Africa. The collective assessment based on the marine proxies ($U_{37}^{K'}$ SST, contents of TOC and chlorins, Upwelling Radiolarian Index and the percentage of *Florisphaera profunda*), surprisingly indicates that the last glacial maximum (LGM) was characterized by warmer sea surface temperature (SST), weaker upwelling, and lower marine productivity, compared with the preceding older glacial and subsequent deglaciation periods. Of the terrigenous proxies, the mean grain size of the non-carbonate fraction and the terrigenous alkane content indicate that wind strength and aridity were high. The weaker upwelling at the 658 site during the LGM may have resulted from changes in the strength and direction of the wind systems and/or shifts in the position and geometry of the upwelling cell. © 2000 Elsevier Science Ltd. All rights reserved.

Keywords: Sea surface temperature; Alkenones; Chlorins; *n*-Alkanes; Compound-specific $\delta^{13}C$; Upwelling

1. Introduction

The eastern tropical Atlantic and Northwest African region has an important but complicated climate system (Fig. 1) that includes the Intertropical Convergence Zone, the low-altitude northeast trade winds (NETW) and the middle-altitude Saharan Air Layer (SAL), a major upwelling cell and the Canary Current. The atmospheric circulation patterns over the coast off NW Africa are dominated by the easterly SAL and the northeasterly NETW. The main upwelling cell is driven by the NETW, thus generating a high productivity zone. Both wind systems contribute terrigenous material to

the marine environment (Tetzlaff and Wolter, 1980; Sarnthein et al., 1981, 1982; Ruddiman et al., 1989). An early study by Sarnthein et al. (1981) indicated that the direction of the SAL remained constant throughout the last 18 kyr, though the speed of this wind system was believed to be lower at the LGM. In contrast, NETW speed was inferred to be higher than today at 18 ka, and presumably with stronger upwelling. Hence, comparing the last glacial with the Holocene, one would expect to find stronger upwelling, higher marine productivity, lower SSTs than predicted on the basis of global glaciation, and higher dust input. Indeed, several studies have concluded that the glacial period was characterized by a more arid NW African continent, stronger winds, and increased upwelling and productivity off NW Africa (Sarnthein et al., 1981, 1982, 1992; Hooghiemstra, 1988). However, most stratigraphic studies have been of insufficient resolution to give a detailed record of the

* Corresponding author. Tel.: +1-603-646-2150; fax: +1-603-646-3922.

E-mail address: meixun.zhao@dartmouth.edu (M. Zhao).

few thousand years around the LGM, when climatic changes could have been both fast and large in this region (Ruddiman et al., 1989; Eglinton et al., 1992). Such changes can be reconstructed using marine sediments at sites such as ODP Site 658 (Fig. 1), which was cored below the main upwelling cell, on the continental slope west of Cap Blanc (20°45'N, 18°35'W; 2263 m water depth). High biological productivity coupled with relatively high terrigenous input has produced high sedimentation rate records containing important paleo-proxy components (Dupont, 1989; Poynter et al., 1989; Ruddiman et al., 1989a,b; Tiedemann, 1991; Winn et al., 1991; Eglinton et al., 1992; Zhao et al., 1993, 1995; Harris and Maxwell, 1995; Chapman et al., 1996; Harris et al., 1996; Jordan et al., 1996; Maslin et al., 1996; deMenocal et al., 2000). In this paper we report several new data sets for core 658C of marine (Upwelling Radiolarian Index, URI) and terrigenous (mean grain size of the non-carbonate fraction; content of *n*-alkanes; $\delta^{13}\text{C}$ of *n*-C₂₉ and C₃₁ alkanes) paleo-proxies and compare them with the previously published data sets,

in order to assess the changes in oceanographic and atmospheric circulation at centennial to millennial resolution over the last 35 kyr (Table 1 and Figs. 2 and 3).

2. Methods

2.1. Age model

In previous publications (e.g. Zhao et al., 1993, 1995), we employed a working age model of this core which was constructed using a high resolution $\delta^{18}\text{O}$ stratigraphy of *Cibicides wuellerstorfi* (Maslin et al., 1996). This stratigraphy was correlated with those of 658A/B and with those of several C-14 dated cores from the N. Atlantic (Winn et al., 1991). However, a very recent paper (deMenocal et al., 2000) gives a radiocarbon-based age model for the last 23.9 calendar ka of 658C, derived from accelerator mass spectrometry (AMS) radiocarbon dating of *Globigerinoides bulloides* over 18 levels, and we have utilized this age model here. It gives

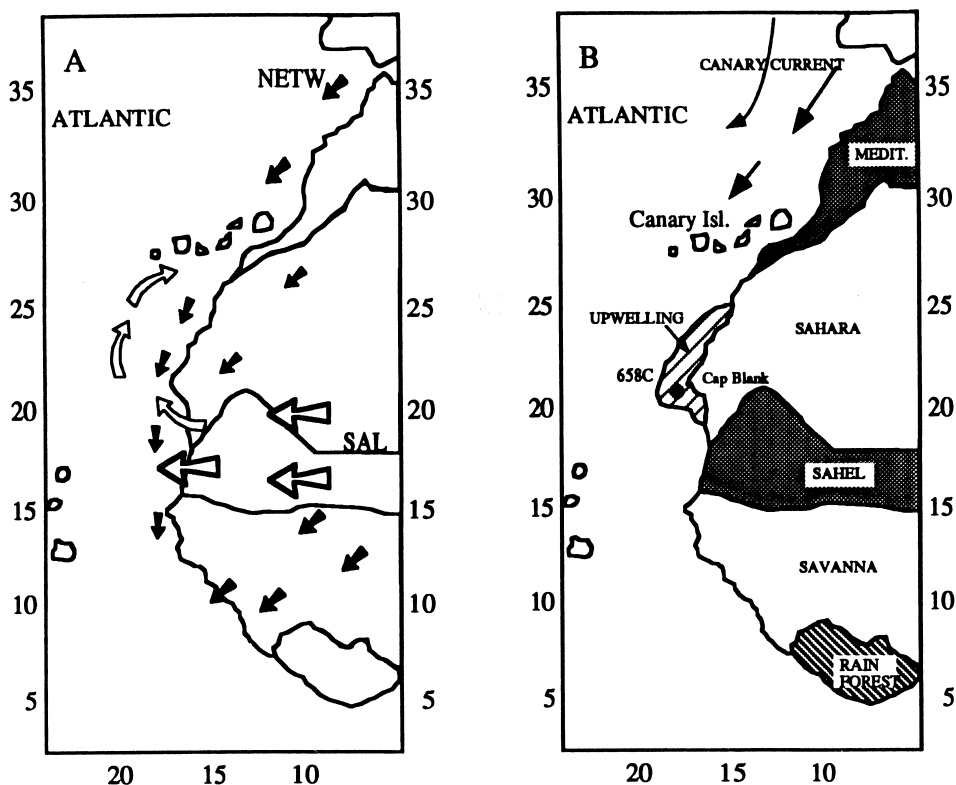


Fig. 1. (A) Present day major wind belts and (B) vegetation zones, surface ocean currents and upwelling region in the northwest African region (modified from Hooghiemstra, 1989). SAL = Saharan Air Layer; NETW = North East Trade Wind; 658C = Site of Ocean Drilling Program Hole 658C. The predominant vegetation types for the zones from north (N) to south (S) are as follows: Mediterranean: Forest (N), and semi-desert, grassland and shrubland (S) — mainly C₃. Sahara: Semi-desert, desert and absolute desert — mainly C₄. Sahel: semi-desert, grassland and shrubland (N), and wooded grassland and deciduous bushland (S) — mainly C₄. Savanna: Sudanian woodland — mixed C₃/C₄. Rain forest: Tropical rain forest — C₃.

Table 1
Summary of average values (bold) and ranges (in parentheses) of paleoenvironmental proxy records for the last 35 kyr divided into five periods

Time zone	Age interval (ka)	SST (U_{37}^K) (°C)	TOC content (%)	Chlorin content ($\mu\text{g g}^{-1}$)	URI (%)	<i>F. profunda</i> (%)	Mean grain size (μm)	Terrigenous content (%)	<i>n</i> -alkane content ($\mu\text{g g}^{-1}$)	$\delta^{13}\text{C}_{29}$ <i>n</i> -alkane (‰)
Late Holocene	6–0	20.6 (18.3–21.5)	2.13 (1.62–2.33)	8.9 (3.9–16.8)	3.8 (1.7–7.2)	22 (8–36)	21 (20–22)	59 (44–62)	1.2 (0.6–1.7)	–28 (–29 to –26)
Early Holocene	10–6	20.9 (19.4–21.5)	1.69 (1.54–1.84)	5.1 (1.7–11.7)	6.9 (4.0–10.5)	26 (10–39)	20 (19–21)	43 (39–48)	0.86 (0.5–1.7)	–27 (–28 to –25)
Deglaciation	18–10	18.7 (17.7–19.6)	1.55 (0.87–1.94)	6.5 (2.4–18.4)	7.0 (4.1–9.5)	9 (3–26)	23 (20–27)	47 (40–58)	0.92 (0.6–2.0)	–25 (–28 to –23)
Last glacial max	22–18	19.6 (18.4–20.3)	0.75 (0.53–0.96)	2.0 (1.0–4.8)	2.9 (1.6–5.4)	16 (7–27)	30 (28–32)	57 (53–59)	0.65 (0.5–0.9)	–24 (–29 to –21)
Older glacial	35–22	18.5 (16.0–19.5)	1.40 (0.60–1.84)	3.8 (1.5–12.2)	3.0 (0.9–4.5)	10 (3–22)	27 (25–30)	60 (54–64)	1.2 (0.5–1.6)	–26 (–26 to –24)

an average sedimentation rate of approximately 18 cm/ka. Beyond 23 ka we have used the same slope to extend to 35 ka. The effect of the deMenocal et al. (2000) age model has been to compress part of the sediment record, previously 18 to 7 ka, into 15 to 7 ka, and to introduce a non-depositional or erosional hiatus from 17.20 to 14.80 cal. ka BP, which is believed to span the first phase of the deglaciation. The 4 cm interval of sediment comprising the hiatus was sampled for some of the proxies but these points have not been included in the plots, since they cannot be assigned ages pending better AMS constraint of the hiatus. The last glacial maximum (LGM) and the Heinrich 2 event remain essentially unchanged in their position on the age plot (Fig. 2B). Our previous interpretations of paleoceanographic changes over the glacial to interglacial period for SST and productivity (Zhao et al., 1995; Harris et al., 1995, 1996) remain largely unchanged by the new age scale.

2.2. Analytical methods

For alkenones and *n*-alkane analyses, a complete suite of U-channel minicores from 658C was sampled at every 2 cm. About 0.5 g of freeze-dried sediment was extracted with solvents and analyzed by GC (Zhao et al., 1995). SST was calculated from the abundances of $C_{37:2}$ and $C_{37:3}$ alkenones (Brassell et al., 1986), using the calibration of Prahl et al. (1988):

$$T(^{\circ}\text{C}) = (U_{37}^{K'} - 0.039)/0.034$$

For the determination of $\delta^{13}\text{C}$ of C_{29} and C_{31} *n*-alkanes, about 5 g of dry sediment was extracted in a sonication bath with 6 ml of DCM:MeOH (3:1 by volume) five times. The supernatants were combined and dried under a stream of nitrogen gas. The residue was fractionated using silica gel column chromatography and the hydrocarbon fraction was measured by GC and GCMS for quantification of concentration and by GC–IRMS for the estimation of $\delta^{13}\text{C}$ values of the C_{29} and C_{31} *n*-alkanes (Collister et al., 1994). Calibration was made with a CO_2 standard introduced at the beginning and end of each GC–IRMS run. Errors for $\delta^{13}\text{C}$ were estimated at $\pm 0.5\text{‰}$.

For coccolith analysis, small spatula-sized samples of core material were taken and examined by smear slide analysis. The counts are represented as species percentage abundance relative to the total coccolith count (Jordan et al., 1996).

Samples for radiolarian analysis were prepared by removing the carbonate fraction with dilute hydrochloric acid and treating the residue with hydrogen peroxide. The $> 63 \mu\text{m}$ fractions were then mounted on glass slides and viewed with a transmitted light stereomicroscope. Radiolarian abundance is expressed as percentage counts. The Upwelling Radiolarian Index

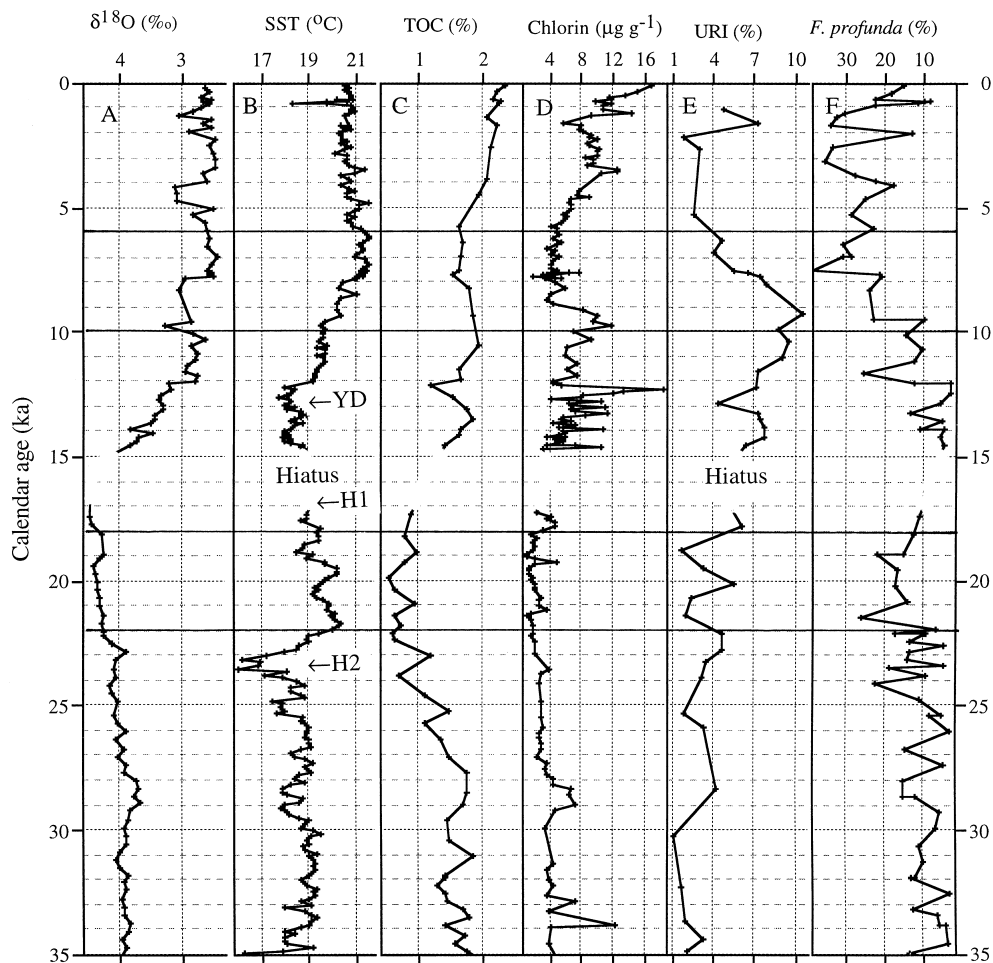


Fig. 2. Marine proxy records for the last 35 kyr at Site 658C. From left to right: (A) $\delta^{18}\text{O}$ of benthic foraminifera *C. wuellerstorfi*; (B) U_{37}^K SST ($^{\circ}\text{C}$); (C) TOC content (% dry weight); (D) chlorin content ($\mu\text{g g}^{-1}$); (E) upwelling Radiolarian Index (%); (F) relative abundance of *F. profunda* (%). The percentage scale is inverted, indicating more turbulent conditions (such as upwelling) to the right (lower%). Data from: A, Maslin et al., 1996; B, Zhao et al., 1995; C&D, Harris et al., 1996; E this paper and F, Jordan et al., 1996. The age scale adopted is that of deMenocal et al., 2000.

(URI) is constructed by summing the percentage abundances of the upwelling assemblage component species (Nigrini and Caulet, 1992; Haslett, 1995; Venec-Peyre et al., 1995; Vergnaud-Grazzini et al., 1995; Haslett and Funnell, 1996), which include *Diptyophimus infabricatus*, *Eucyrtidium erythromystax*, *Lamprocyclus hadros*, *Lamprocyclus maritimalis ventricosa*, *Pterocanium grandiporus*, *P. auritum*, *Acrosphaera murrayana*, *Lithostrobis* cf. *L. hexagonalis*, *Phormostichoartus caryoforma*, *P. crustula*, *Pterocorys minythorax* and *Lamprocyrtis nigriniae*.

The method for the chlorin analysis has been reported in Harris et al. (1996), while the grain size measurement was done with a Sedigraph and has been described in detail by Beveridge (1994).

3. Results and discussion

3.1. Marine proxies

The marine proxy records for the last 35 kyr are presented in Fig. 2 and summarized in Table 1. The records are divided into five time spans: older glacial (22–35 ka), LGM assigned as 18–22 ka (There is still no single, internationally recognized duration for the LGM: it is now defined by EPILOG as 19–23 cal. ka, but 18–22 cal. ka by German GLAMAP-2000), deglaciation (10–18 ka), early Holocene (6–10 ka) and late Holocene (0–6 ka). The $\delta^{18}\text{O}$ ‰ record for the benthic foraminiferum *Cibidoides wuellerstorfi* (Fig. 2A) is from Maslin et al.

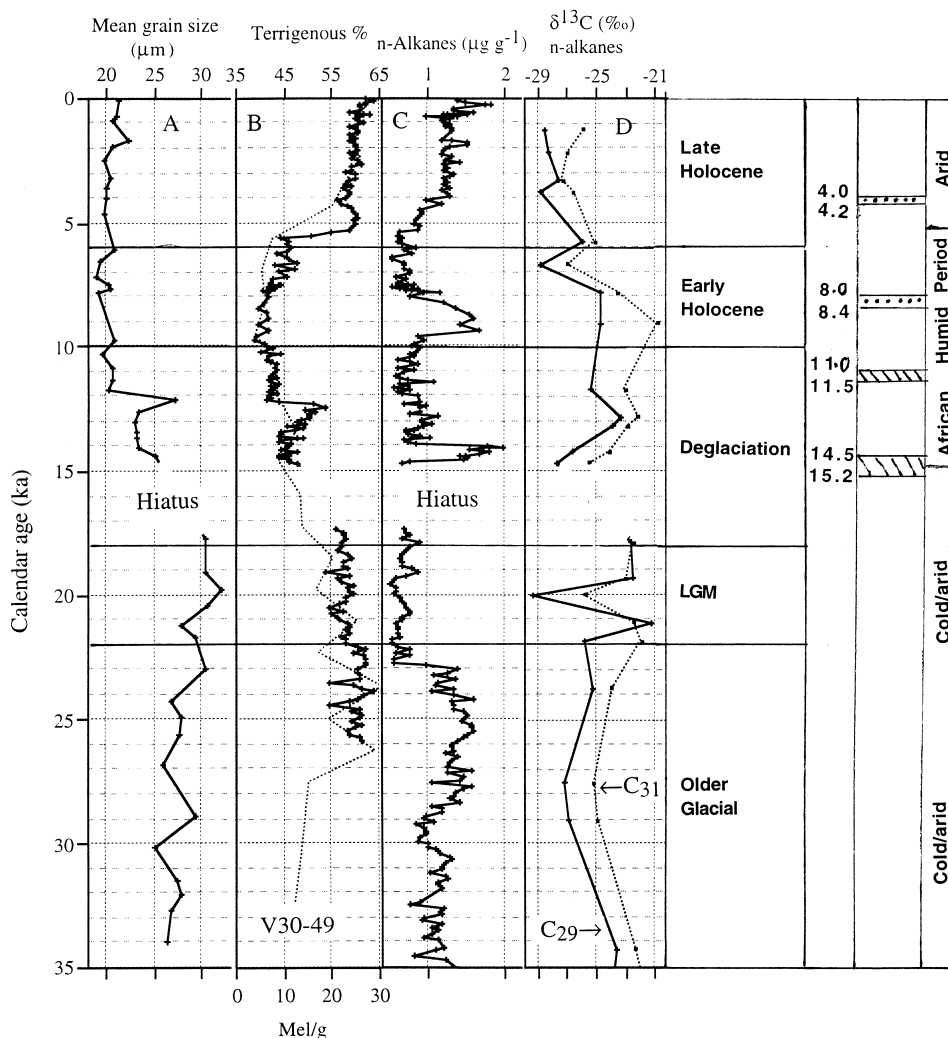


Fig. 3. Terrigenous proxy records measured for 658C. From left to right: (A) mean grain size of the 64–10 μm non-carbonate fraction; (B) terrigenous% (solid line, deMenocal et al., 2000) and the abundance of the fresh water diatom *Melosira* in core V30-49 ($18^{\circ}26'N$, $21^{\circ}05'W$) (dotted line, Alan Mix, personal communication); (C) *n*-alkane content ($\Sigma C_{27}, C_{29}, C_{31}, C_{33}$) ($\mu\text{g g}^{-1}$); (D) $\delta^{13}\text{C}$ (‰) of C_{29} *n*-alkane (solid line) and of C_{31} *n*-alkane (dotted line). The age scale adopted is that of deMenocal et al. (2000). The climatic assignments in the right hand columns are from Gasse (2000); the hatched intervals (cal. ka BP) indicate exceptionally wet and warm periods and the dotted intervals (cal. ka BP) indicate unusually dry periods or transitions in NW Africa. The timing of the African Humid Period (14.8–5.5 cal. ka BP) is from deMenocal et al. (2000).

(1996), replotted on the deMenocal et al. (2000) age scale.

The U_{37}^K SST record (Fig. 2B) has varied by 6°C over the last 35 kyr. The lowest SST of 16°C around 23–24 ka is believed to be associated with Heinrich event 2 cooling of the N. Atlantic Ocean (Bond et al., 1993). Meltwater produced by these ice-rafting events would seem to have been transmitted southward by the Canary Current, where it had considerable impact on sea surface temperature in the subtropical eastern Atlantic (Zhao et al., 1995). The regions corresponding to the Younger Dryas (ca. 12.3 cal. ka BP) and to Heinrich

event 1 (ca. 17.5 cal. ka BP) are also indicated in Fig. 2B, although the latter falls at the lower boundary of the hiatus for 658C. The glacial/interglacial U_{37}^K SST difference of 2.4°C is in agreement with other SST estimates for this region (Mix et al., 1986). The most interesting feature is that the lowest SST was not recorded during the LGM. In fact, the average LGM SST was $\sim 1^{\circ}\text{C}$ higher than those of the older glacial and the deglaciation. The immediate question to ask is what caused the SST increase during the LGM. Variations of 658C SST can be influenced by upwelling and surface currents in addition to the global glacial/interglacial signature.

Globally, the continents and major oceanic regions experienced the lowest temperatures during the LGM (Jouzel et al., 1987; Bond et al., 1993), but the LGM was not the lowest SST period during the glacial stage everywhere. Temperatures in the North Atlantic were influenced by Heinrich events, when SSTs were markedly colder in a number of areas. For example, at the site of a northeast Atlantic core (48°23'N, 25°05'W), Madureira et al. (1997) found that the SSTs were lowest in stage 3 at Heinrich 4, at a second minimum during H2 and then immediately rose at the beginning of the LGM. In the South Atlantic the lowest SSTs appeared in mid stage 3 (Muller et al., 1994; Schneider et al., 1995). At site 658, we infer that the upwelling decreased substantially and/or that warm tropical surface water invaded this region. We have therefore used additional proxy records to evaluate past changes in upwelling strength.

The URI (Fig. 2E) provides an independent means of estimating relative upwelling intensity, high values corresponding to stronger upwelling (Nigrini and Caulet, 1992; Haslett, 1995). Nevertheless, upwelling can increase without affecting SST, where cold water fails to reach the surface. URI values for 658C range from 1 to 10, confirming that upwelling has persisted over the last 35 kyr. URI for the older glacial and the LGM was low but variable, evidencing that upwelling was relatively weak with short periodic increases. Upwelling increased at the onset of the deglaciation and remained high until 8–9 ka, when it began to decrease and stayed relatively low during the rest of the Holocene. The low upwelling during the LGM is in accord with the warmer U_{37}^K SST, while the inferred stronger upwelling just prior to 8–9 ka matches the lower SSTs which persisted into the early Holocene. The SST would have been higher during the early Holocene without this period of strong upwelling.

The relative abundance of the coccolithophorid alga *Florisphaera profunda* (%) (Fig. 2F) provides an index of the extent of surface water stratification, which can be regarded as an inverse index of upwelling intensity (Molfin and McIntyre, 1990; Jordan et al., 1996). This species is restricted to the lower euphotic zone and requires stable surface water conditions to grow: high values correspond to well-stratified photic zones with a deep nutricline and thermocline while low values reflect turbulent conditions, such as those occurring during upwelling. The *F. profunda* abundance in Fig. 2F is in part consistent with the SST and URI records. Low values, corresponding to strong upwelling and hence low SSTs, are particularly noticeable during the deglaciation. There are discrepancies, e.g. some relatively high *F. profunda* values correspond to the high URI values in the early Holocene. These slightly out-of-phase relationships are common in paleoceanography, and may be due to taphonomic processes (e.g. bioturbation may sort big radiolarian from small nannofossils over several centimetres).

The TOC record (Fig. 2C; Müller and Suess, 1979; Sarnthein et al., 1992) and that of the content of chlorins (Fig. 2D; Harris et al., 1996) can be used as independent measures of marine productivity. Both records indicate somewhat lower marine productivity during the older glacial and especially the LGM, followed by increased productivity during the deglaciation. A reduction in marine productivity does not necessarily reflect a decrease in upwelling strength, since other factors also influence productivity. Diagenesis can be expected to result in a weak overall downhole trend to lower values for TOC and chlorin content with increasing core depth. Such effects may in part explain the trends to lower values apparent with increasing age in the Holocene section. Part of the increase in productivity in the early Holocene may have been due to the short-term fertilizing effect of wadi discharge, such as that observed in the Eemian (Tiedemann, 1991), and of the increased river input which seems to have occurred during most peak interglacial stages at site 658 (Westerhausen et al., 1993). However, a reduced upwelling based on a reduction of productivity at the LGM is at least consistent with the records of the URI and of *F. profunda*.

3.2. Terrigenous proxies

The terrigenous proxy records are presented in Fig. 3 and summarized in Table 1.

Mean grain size (Fig. 3A) can be used as a proxy for assessing paleo-wind systems (Sarnthein et al., 1982). The situation at site 658 is complicated by the occasional input of fluvial sediment (advected in the nepheloid layer), which is difficult to assess and separate quantitatively from the siliciclastic fraction, particularly during the earliest Holocene and other peak interglacial stages (Tiedemann, 1991). However, as a first approximation, the higher values of mean grain size in 658C sediments near the LGM indicate that total wind speed was higher and/or that the dust source regions were more arid. Higher wind speed and hence increased upwelling is in agreement with previous studies (Sarnthein et al., 1981, 1982), but contrary to the assessments derived from the marine records in Fig. 2.

The terrigenous sediment record shown in Fig. 3B represents the residual sediment percentage obtained after subtraction of the carbonate and opal values (deMenocal et al., 2000). deMenocal et al. (2000) take this fraction as being largely eolian in origin and point out that its high content in the older glacial abruptly decreases at 14.8 cal ka BP (though this timing is not at present stratigraphically distinguishable from the hiatus), a date which agrees well with the onset of the African Humid Period. The terrigenous/eolian percentage rises and falls again over ca. 2 ky around the time of the Younger Dryas (placed here at 12.3 cal ka BP) and then abruptly increases at ca. 5.5 cal ka BP and

stays high for the rest of the Holocene. This last abrupt rise corresponds with the termination of the African Humid Period and the rapid onset of more arid conditions in north Africa. These transitions apparently occurred with great rapidity, within decades to centuries, and deMenocal et al. (2000) propose that they were driven by two positive feedback mechanisms (coupled vegetation/albedo and SST/moisture transport) which are assumed to interact with the primary insolation forcing “to lock the subtropical African climate into one of two (vegetated versus non-vegetated) stable equilibrium climate conditions” (Claussen et al., 1998). The similar trend of grain size and terrigenous % for the period 27–13 ka BP indicates that the increased terrigenous content during the glacial time could be caused by both aridity and wind strength. However, the late Holocene increase in terrigenous% is correlated with lower grain size values, which implies that aridity was responsible for this terrigenous increase. Independent paleohydrological data (lake, groundwater and speleothem records) for north Africa, reviewed by Gasse (2000), also reveal major abrupt climatological changes (Fig. 3) since the LGM, namely (1) a wetting/warming phase at 17–16 ka BP, (2) two drastic arid to humid transitions around 15.2–14.5 and 11.5–11 ka BP (which resulted in a wet and green Sahara), and (3) major dry spells around 8.4–8.0 and 4.2–4.0 ka BP, followed by generally arid conditions until the present day.

The contents of long-chain *n*-alkanes (C_{27} , C_{29} , C_{31} and C_{33} ; Fig. 3C) also represent the terrigenous input into marine sediments. These biomarkers are specific to higher land plant leaf waxes (Eglinton and Hamilton, 1967) and are in eolian dust (e.g. Simoneit et al., 1977; Gagosian et al., 1981; Huang et al., 1993, 2000) and fluvial particulates (Bird et al., 1995; Pelejero et al., 1999). The content of the *n*- C_{29} homologue, non-acosane, has been used in several marine stratigraphic studies as a proxy for leaf wax input. Thus, Poynter et al. (1989a,b), Ishiwatari et al. (1994) and Madureira et al. (1997) interpreted its variations through time in terms of changing terrigenous input related to wind strength. In the cores studied, the content of *n*- C_{29} was high in glacial times, in parallel with higher percentages of terrigenous sediment and consistent with a higher input of dust during the cold, windy and arid conditions at that time. For site 658, dust inputs were more important during the arid glacial period, while riverborne particles might be expected to contribute significantly during the warmer and more humid early Holocene period (deMenocal et al., 2000). Advection processes can also be important. Thus, Bertrand et al. (1996) suggested that the organic carbon flux at a nearby site (11 k, in the same upwelling area but considerably nearer the shoreline) increased from the last glacial to the present interglacial as a result of advection of sediments from the shelf as it extended inland with

sea level rise. In another core study at a site in the southern South China Sea, the highest erosional input of both clays and *n*-alkanes occurred at times of low sea level stand, 23 to 14 cal. ka BP, when a large area (Sundaland) and a drainage system, the Molengraaff River, developed in the emergent tropical lowland (Pelejero et al., 1999). However, the 658C site would still be far from land at the last glacial maximum. In the 658C record the content of *n*-alkanes (Fig. 3C) does not parallel the mean grain size proxy (Fig. 3A) for wind strength/aridity or the terrigenous % (eolian) records (Fig. 3B). The content of *n*-alkanes was high during the later half of the older glacial, but was low during the LGM. The explanation may lie in there being at least two main source regions for the dust reaching 658C: Europe, the Mediterranean, the northern Sahara and the NW African coastal region for the NETW; and the central and southern Sahara and the Sahel for the SAL (Dupont, 1989). For each region, the loads of leaf wax alkanes and inorganic mineral grains can be expected to vary selectively, dependent on the wind strength/direction, the aridity and the extent and nature of the local vegetation cover.

The $\delta^{13}C$ values (Fig. 3D) of the long chain *n*-alkanes studied reflect the type of CO_2 fixation mechanism adopted by the originating plants, namely, C_3 or C_4 plants; CAM plants, which are not major components of the NW African vegetation have not been considered further in this paper (Farquhar et al., 1989; Collister et al., 1994). We have measured $\delta^{13}C$ for the most abundant individual *n*-alkanes, C_{29} and C_{31} in the 658C sediments. The $\delta^{13}C$ value for the *n*- C_{31} alkane (Fig. 3D) essentially parallels that of the *n*- C_{29} alkane, in agreement with their common biosynthetic origin, as has been observed in a number of studies (Huang et al., 1993, 1999, 2000; Bird et al., 1995; Yamada and Ishiwatari, 1999). The difference between the two profiles is usually less than 1‰, with *n*- C_{31} more negative (Yamada and Ishiwatari, 1999). Either homologue can be used for compound specific carbon isotope stratigraphy, but we have selected *n*- C_{29} ; unfortunately, our sampling resolution is low compared with those for the other proxies and allows only limited interpretation. However, the 8‰ variation in the compound-specific $\delta^{13}C$ values over the last 35 kyr represents major changes in the relative input of C_3 versus C_4 -derived alkanes. This contrasts with the small, ca. 1‰, variation over the last 27 kyr in the $\delta^{13}C$ values (average $-19.2‰ \pm 0.6‰$, $n=10$) for the TOC, which is dominated by marine organic matter and shows no systematic glacial/interglacial trend.

Few compound-specific $\delta^{13}C$ studies of plant leaf waxes are available as yet, but as a working basis, we assign $-36‰$ for the *n*- C_{29} alkane of C_3 plants and $-21‰$ for the *n*- C_{29} alkane of C_4 plants (Collister et al., 1994). The isotopic values of plant wax *n*-alkanes reflect not only the photosynthetic mechanisms but also the $\delta^{13}C$ of the ambient carbon dioxide fixed and the physiological

responses of the plants to the environmental conditions. However, changes in the concentration and $\delta^{13}\text{C}$ of atmospheric CO_2 over the last 35 kyr (Leuenberger et al., 1992) are unlikely to have had major effects on the $\delta^{13}\text{C}$ of the leaf wax *n*-alkanes. Tree leaf cellulose $\delta^{13}\text{C}$ values were ca. 1‰ heavier in the last glacial, though the response to the ca. 100 ppmv lower CO_2 concentration can be expected to have varied somewhat among C_3 species (Van de Water et al., 1994; Feng and Epstein, 1995). By contrast, C_4 species, such as many grasses (graminae) which populate the savanna, are relatively insensitive to changes in the partial pressure of atmospheric CO_2 and become more widespread at the time of the lower ambient CO_2 concentration of the last glacial (Street-Perrott et al., 1997). The $\delta^{13}\text{C}$ values of *n*-alkanes in sediments reflect the summation of terrigenous plant inputs. Thus, in regard to the eolian input, the present vegetation of the SAL dust source region is mainly C_4 , while that of the NETW region is mostly C_3 (Hooghiemstra, 1988; Dupont and Agwu, 1991) (Fig. 1). There are no direct measurements of the $\delta^{13}\text{C}$ values of *n*-alkanes from pure SAL- and/or NETW-carried dusts. However, Simoneit (1997) found that the *n*- C_{29} alkane component of aerosols collected in northern Nigeria under Harmattan conditions had values of -29.2‰ (-26.6 to 30.1‰ , seven samples). The sources of these *n*-alkanes were inferred to include the vegetation of submontane savanna, shrubs and forest, and also, soil organic matter (e.g. -30.7‰) carried by the northeasterly Harmattan wind towards the equatorial East Atlantic and Gulf of Guinea. Other components of such tropospheric aerosol loads include products of biomass burning, such as the abundant carbonaceous particles (mainly $<1\ \mu\text{m}$ size) reaching the Ivory Coast region (Cachier et al., 1985; Bird and Cali, 1998). These carbonized particles reveal $\delta^{13}\text{C}$ bulk values affected by the burning processes, but pyrolytic fractionation is unlikely to change the $\delta^{13}\text{C}$ values of individual *n*-alkane components.

Finally, $\delta^{13}\text{C}$ *n*-alkane mapping of marine surface sediments over a wide region off NW Africa stretching from Portugal south to the Gulf of Guinea clearly shows that areas in the main track of the NETW have more negative *n*-alkane $\delta^{13}\text{C}$ values than areas directly beneath the SAL (Huang et al., 1993, 2000). For example, nearby to site 658 at $\sim 20^\circ\text{N}$, where the SAL dust input predominates, the $\delta^{13}\text{C}$ value of *n*- C_{29} is around -26.2‰ , indicating ca. 50% C_4 contribution. Further north (36°N) and south (1°S), the values reach -32‰ , indicating predominantly C_3 contributions.

3.3. Vegetational changes of source regions

Several pollen studies have indicated that the vegetation of NW Africa has experienced major changes throughout the last glacial/interglacial cycle (Hooghiemstra, 1988, 1989). Based on chenopod pollen, it would appear that

the Sahara expanded in both north and south directions during the LGM. The NETW intensified, especially between 36 and 24°N , and took western Mediterranean trade wind indicator pollen as far south as 10°N , while the SAL had a stationary position over site 658 between 17 and 21°N . Between 22 and 16°N the marine pollen record registered changes in both the vegetation of the western Mediterranean area and of the gramineae vegetation of the savanna region in the south. In contrast, in the middle Holocene, following the African Humid Period and prior to about 4 ka BP, geomorphic and biostratigraphic evidence has revealed that NW Africa was extensively vegetated. Lakes were present as far north as 27°N and grasslands to 23°N , while no desert plants reached further south than 20°N (Joussaume et al., 1999).

Some idea of the aridity history of the NW African hinterland has been gained from the marine record of the freshwater diatoms of the genus *Melosira*. The tests of these diatoms reach the Atlantic following deflation of diatomaceous deposits in dry lake beds of the Sahara. Pokras and Mix (1985) pointed out that the counts of these provide an indication of the continental lake levels and therefore of aridity. A portion of their “aridity curve for tropical NW Africa”, obtained with core V30-49 ($18^\circ 26'\text{N}$, $21^\circ 05'\text{W}$, close to 658C) is shown in Fig. 3B. The site lies beneath the same summer dust plume as does 658C, for which the sources are the western and central Sahara and its borders. This curve and that of the terrigenous% for 658C of deMenocal et al. (2000) (Fig. 3B) run broadly in parallel, as might be expected.

Climatic aridity results in sparse vegetation cover and consequently lower plant biomass and a reduced amount of contemporary, freshly biosynthesized leaf wax available for wind transportation. The leaf wax load carried by the wind systems out to the ocean will, of course, also contain older, sedimentary leaf waxes which have been lifted off in the dust from dried-up lake beds and areas of desiccated soils. This load will depend rather crucially on the aridity, since deflation of dust is highly dependant on the moisture content of the soil being eroded (Pye, 1987). Hence, the relationship between aridity in the Sahel/Sahara and the eolian supply of leaf waxes (alkane contents) to site 658C sediments is likely to depend non-linearly on these two inputs — the supply of “old” alkanes in deflated dust and of “young” alkanes from contemporary vegetation — both somewhat proportional to wind strength. The “old” alkane supply can be expected to be high when the aridity is high, but the actual load carried by the winds will also depend on which soil horizons or lake sediment layers are being eroded at the time. Rapid erosion of organic-rich horizons such as top soils will give dust of high alkane content which may then be followed by erosion of organic-lean, older, deeper layers of sediments or soils, affording dust of lower alkane content. Such a scenario taking place over an extended area like the

Sahara and the Sahel could provide significant quantities of *n*-alkane to the marine sedimentary record. In view of the major dry spell at 4.2–4 cal. ka BP (Gasse, 2000) and the ensuing aridity until the present day (Fig. 3), the generally higher level of alkane content after 4 ka (Fig. 3C) may have been generated in this way. The “young” alkane supply can be expected to decrease with increasing aridity as vegetation cover decreases. However, qualitatively, there must be a counter effect of increased abrasion and deflation of leaf waxes from leaf surfaces with increasing dust load in the surface winds. Thus, one might expect an increase in leaf wax supply to the marine sediments when the African Humid Period (14.8–5.5 cal. ka BP; deMenocal et al., 2000) had proceeded far enough to substantially increase the vegetation cover of large areas of the Sahara and the Sahel; the peak at ca. 14.5 ka BP might have been generated in this way. Abrupt interruption of such a humid phase by an arid period might then result in massive vegetative die-back and increased erosion of newly desiccated sediments carrying a high load of leaf waxes. The peak in the *n*-alkane record around 9–8 ka might have such an explanation, in view of the major dry spell from 8.4 to 8 ka documented by Gasse (2000).

Similar considerations apply to the *n*-C₂₉ δ¹³C ‰ record. Aridity affects both the amount of vegetation and its photosynthetic type. The proportion of C₃ vs. C₄ plants will respond to changes in climatic conditions, with consequences for the δ¹³C ‰ values of the *n*-alkanes and the composition of the pollen transported to the marine sediments. If we assume that other sources (river, etc.) are not generally significant, then downcore alkane δ¹³C ‰ records can be interpreted in terms of temporal changes in C₃ versus C₄ plant input (Huang et al., 1993; Bird et al., 1995) and therefore, as a first approximation, the relative fluxes from NETW (mainly C₃) and SAL (mainly C₄). However, winds can pick up C₄ and C₃-laden dust in a time variable way, dependent on shifts in aridity and in vegetation zones consequent upon climatic change in the dust source areas. The average δ¹³C value of ca. –28‰ (Fig. 3D, Table 1) for the C₂₉ *n*-alkane in the late Holocene is close to that (–26.3‰) of core top sediments near the 658 site (Huang et al., 2000), equating with similar contributions from C₃ and C₄ plants, in agreement with modern observations that this area receives dust inputs from both SAL and NETW (Sarnthein et al., 1981). The older glacial value for *n*-C₂₉ is about –26‰. However, in the LGM δ¹³C appears to oscillate markedly around ca. –24‰, one sample being as light as –29‰ and another as heavy as –21‰, a value like that for the *n*-C₂₉ alkane of modern C₄ plants (Farquhar et al., 1989; Collister et al., 1994); the CO₂ concentration effect may possibly account for 1‰ of this shift (see above). One explanation for the heavy values would require that increased aridity of the NETW source region resulted in a shift to a C₄-dominated ecosystem. However, pollen

data indicate that the glacial floral community of the northwest African and west Mediterranean region was not greatly different from that of the Holocene, though it was more sparse and of more limited distribution (Hooghiemstra, 1988; Dupont, 1989).

3.4. Paleoclimatic and paleoecological implications

Complex natural situations are intrinsically difficult to study and generally require application of information derived from a number of parameters. Thus a multi proxy study, such as that used in the present paper, benefits from the application of a number of proxies which reflect a phenomenon in common, such as upwelling. However, this approach, while superficially appropriate, may be fraught with difficulties. Thus, SST is not an independent indicator of upwelling, since it may be influenced dramatically by changes in current systems. Furthermore, the U_{37}^K proxy for SST is not simply a measure of temperature at the sea surface but depends on the originating organisms and their responses to seasonal conditions, such as nutrient concentrations. Indeed, most proxies are dependant on a variety of biological and physico-chemical factors. They are nonetheless useful when employed together to study complex situations such as sedimentary records, but they cannot be expected to provide a single, unambiguous interpretation; the differences which emerge may prove highly informative when the operation of the proxies is better understood (Eglinton et al., 2000). In the present paper the marine proxy records are only in part agreement with each other. Thus, the URI% is highest at ca. 9 ka while U_{37}^K SST is warm. Again, comparing URI% and *F. profunda*%, URI is moderately high in the late deglaciation while *F. profunda* is at its lowest. Comparing all of the marine proxies over the late Holocene, TOC and chlorin contents and *F. profunda*% are moderate to high, suggestive of fairly active upwelling (indeed, site 658 is in the main upwelling cell today) while URI% are low and U_{37}^K SST are high, in accord with weak upwelling. These apparent contradictions make it difficult to arrive at firm generalizations. They may arise in part from the lower resolution sampling of some of the proxies, e.g. URI and *F. profunda*, differential bioturbation and diagenesis of sediment components and the overall complex nature of the determining factors. For example, the varying input of terrigenous versus marine organic matter will affect TOC%, while in the case of *F. profunda*%, the relationship between stratification and upwelling is rather uncertain. However, in spite of the difficulties with the 658C record, what does emerge is that the marine proxies indicate reduced upwelling during the LGM, followed by an increase during the deglaciation stage.

Turning to the terrigenous proxies, the low amounts of *n*-alkanes (Fig. 3C) deposited at the LGM can be

interpreted in terms of decreased wind strength, again implying reduced coastal upwelling. But the $\delta^{13}\text{C}$ ‰ data (apart from the data point at 20 cal. ka BP) indicate a C_4 dominated input, and on this basis, the input of dust to ODP site 658 during the LGM was mainly from the C_4 -rich SAL, rather than from the C_3 -rich NETW. The African continent is held to be much drier at the LGM (Sarnthein et al., 1982; Hooghiemstra, 1988, 1989; Dupont, 1989) and hence both wind systems would be expected to deflate more dust. A relative reduction in NETW dust input could be the result of reduced NETW speed, with or without changes in its direction, while a relative increase in the C_4 load would require changed vegetation cover of the NETW source region toward C_4 domination. Both scenarios seem unlikely, based on the pollen and sedimentological evidence (e.g. Hooghiemstra, 1988, 1989; Dupont, 1989) but the latter would allow the NETW to be strong during the LGM. There is clearly a problem. One explanation may lie in terms of our data being from one site only. Since coastal upwelling is largely a local phenomenon, changes in both wind direction and sea level could have influenced the spatial distribution of upwelling strength. At the LGM, Site 658 might not have been centrally placed in the main upwelling cell. In which case, other nearby regions might have received more NETW dust load and experienced more upwelling (Bertrand et al., 1996). However, the warming of SST at the LGM was not confined to Site 658. More regionally, Mix et al. (1986) have reported data for other sites in the tropical N. Atlantic that had relatively warmer SSTs during the LGM and colder SSTs centered in the deglaciation. In summary, the two terrigenous proxies, *n*-alkane content and $\delta^{13}\text{C}$ ‰ of *n*- C_{29} , show abrupt changes which are likely significant but not readily interpreted. Both proxies must be highly dependent on the nature and geographical extent of the vegetation cover which is, in turn, dependent on aridity, temperature, insolation and ambient CO_2 concentrations. Higher resolution sampling across important time horizons, such as those displaying major shifts in both alkane content and $\delta^{13}\text{C}$ ‰ of *n*- C_{29} at this and other sites in the 658 area will be needed to further resolve this situation. The 658C multi proxy record and the links between marine phenomena, such as upwelling, and continental conditions, such as aridity, wind strength and vegetation cover will be addressed in greater detail over two full glacial and interglacial cycles (last 250 ky) in a future publication (Zhao et al., in preparation).

4. Conclusions

Five marine proxy records for 658C over the last 35 ky accord with somewhat reduced upwelling at this site during the LGM. However, only one terrigenous proxy,

the *n*-alkane content, accords with weak eolian dust transport, while two others, mean grain size and terrigenous sediment%, indicate strong winds at this time, and hence, strong upwelling. This contradiction may have a variety of explanations which cannot be tested with the present data set including, for example, changes in the strength and direction of the NETW/SAL wind systems, and/or changes in the position and geometry of the upwelling cell due to current shifts.

Acknowledgements

We thank N. Beveridge for the grain size measurements, P. Harris and J.R. Maxwell for the chlorin data, Ann McNichol for the TOC $\delta^{13}\text{C}$ data, M. Teece for some GC-IRMS data, Alan Mix for *Melosira* data for core V30-49 and Peter deMenocal for the 658C age scale and the terrigenous content data. We thank J. Carter and G. Read for technical help, the Organic Geochemistry Mass Spectrometry Facility for access, the Natural Environment Research Council and the European Community for financial support (GST/02/553 and EV5V-CT-92-0117). We thank Dr. L. Labeyrie for the U-channel tubes, the ODP for samples, and Drs. J. Grimalt and C. Pelejero and two anonymous referees for their helpful comments. The data sets will be available from the Pangea database.

Associate Editor—J. Grimalt

References

- Bertrand, P., Shimmield, G., Martinez, P., Grousset, F., Jorissen, F., Paterne, M. et al. (Participants of the Sedorqua Program), 1996. The glacial ocean productivity hypothesis: the importance of regional temporal and spatial studies. *Marine Geology* 130, 1–9.
- Beveridge, N.A.S., 1994. Palaeoceanography of the Eastern Atlantic. PhD thesis, University of Cambridge.
- Bird, M.I., Summons, R.E., Gagan, M.K., Rokсандic, Z., Dowling, L., Head, J. et al., 1995. Terrestrial vegetation change inferred from *n*-alkanes $\delta^{13}\text{C}$ analysis in the marine environment. *Geochimica et Cosmochimica Acta* 59, 2853–2857.
- Bird, M.I., Cali, J.A., 1998. A million-year record of fire in sub-Saharan Africa. *Nature* 394, 767–769.
- Bond, G., Broecker, W., Johnsen, S., McManus, J., Labeyrie, L., Jouzel, J., Bonani, G. et al., 1993. Correlation between climate records from North Atlantic sediments and Greenland Ice. *Nature* 365, 143–147.
- Brassell, S.C., Eglinton, G., Marlowe, I.T., Pflaumann, U., Sarnthein, M., 1986. Molecular stratigraphy: a new tool for climatic assessment. *Nature* 320, 129–133.
- Cachier, H., Buat-Menard, P., Fontugne, M., Rancher, J., 1985. Source terms and source strengths of the carbonaceous aerosol in the tropics. *Journal of Atmospheric Chemistry* 3, 469–489.

- Chapman, M.R., Shackleton, N.J., Zhao, M., Eglinton, G., 1996. Faunal and alkenone reconstruction of subtropical North Atlantic paleotemperature and surface hydrography of the last 28 ka. *Paleoceanography* 11, 343–357.
- Claussen, M., Brovkin, V., Ganopolski, A., Kubatzki, C., Petoukhov, V., 1998. Modeling global terrestrial vegetation–climate interaction. *Philosophical Transactions of the Royal Society of London*, 353B.
- Collister, J.W., Rieley, G., Stern, B., Eglinton, G., Fry, B., 1994. Compound-specific $\delta^{13}\text{C}$ analysis of leaf lipids from plants with differing carbon dioxide metabolism. *Organic Geochemistry* 21, 619–627.
- deMenocal, P., Ortiz, J., Guilderson, T., Adkins, J., Sarnthein, M., Baker, L. et al., 2000. Abrupt onset and termination of the African humid period: rapid climate responses to gradual insolation forcing. *Quaternary Science Reviews* 19, 347–361.
- Dupont, L.M., 1989. Palynology of the last 680,000 years of ODP site 658 (off NW-Africa): fluctuations in paleowind systems. In: Leinen, M., Sarnthein, M. (Eds.), *Paleoclimatology and Paleometeorology: Modern and Past Patterns of Global Atmospheric Transport*. Kluwer Academic Publishers, London, pp. 779–794.
- Dupont, L.M., Agwu, C.O.C., 1991. Environmental control of pollen grain distribution patterns in the Gulf of Guinea and offshore NW-Africa. *Geologische Rundschau* 80, 567–589.
- Eglinton, G., Hamilton, R.J., 1967. Leaf epicuticular waxes. *Science* 156, 1322–1335.
- Eglinton, G., Bradshaw, S.A., Rosell, A., Sarnthein, M., Pflaumann, U., Tiedemann, R., 1992. Molecular record of secular sea surface temperature changes on 100-year time-scales for glacial terminations I, II and IV. *Nature* 356, 423–426.
- Eglinton, T. et al. Collected papers from workshop on alkenone-based paleoceanographic indicators. G-cubed (special issue), submitted for publication (www.g-cubed.org).
- Farquhar, G.D., Ehleringer, J.R., Hubick, K.T., 1989. Carbon isotope discrimination and photosynthesis. *Annual Review of Plant Physiology and Plant Molecular Biology* 40, 503–537.
- Feng, X., Epstein, S., 1995. Carbon isotopes of trees from arid environments and implications for reconstructing atmospheric CO_2 concentrations. *Geochimica et Cosmochimica Acta* 59, 2599–2608.
- Gagosian, R.B., Peltzer, E.T., Zafriou, O.C., 1981. Atmospheric transport of continentally derived lipids to the tropical North Pacific. *Nature* 291, 312–314.
- Gasse, F., 2000. Hydrological changes in the African tropics since the last glacial maximum. *Quaternary Science Reviews* 19, 189–211.
- Harris, P.G., Maxwell, J.R., 1995. A novel method for the rapid determination of chlorin concentrations at high stratigraphic resolution in marine sediments. *Organic Geochemistry* 23, 853–856.
- Harris, P.G., Zhao, M., Rosell-Mele, A., Tiedemann, R., Sarnthein, M., Maxwell, J.R., 1996. Chlorin accumulation rate as a proxy for Quaternary marine primary productivity. *Nature* 383, 63–65.
- Haslett, S.K., 1995. Mapping Holocene upwelling in the eastern equatorial Pacific using Radiolaria. *The Holocene* 5, 470–478.
- Haslett, S.K., Funnell, B.M., 1996. Sea-surface temperature variation and palaeo-upwelling throughout the Plio-Pleistocene Olduvai subchron of the eastern equatorial Pacific: an analysis of radiolarian data from ODP sites 677, 847, 850 and 851. In: Mogailevsky, A., Whately, R. (Eds.), *Microfossils and Oceanic Environments*. University of Wales, Aberystwyth Press, pp. 155–164.
- Hooghiemstra, H., 1988. Changes of major wind belts and vegetation zones in NW Africa 20,000–5,000 yr BP., as deduced from a marine pollen record near Cap Blanc. *Review of Palaeobotany and Palynology* 55, 101–140.
- Hooghiemstra, H., 1989. Variations of the NW African trade wind regime during the last 14,000 years: changes in pollen flux evidenced by marine sediment records. In: Leinen, M., Sarnthein, M. (Eds.), *Paleoclimatology and Paleometeorology: Modern and Past Patterns of Global Atmospheric Transport*. Kluwer Academic Publishers, London, pp. 733–770.
- Huang, Y., Collister, J.W., Chester, R., Eglinton, G., 1993. Molecular and $\delta^{13}\text{C}$ mapping of eolian input of organic compounds into marine sediments in the Northeastern Atlantic. In: Øygard, K. (Ed.), *Organic Geochemistry*. Falch Hurtigtrykk, Oslo, pp. 523–528.
- Huang, Y., Street-Perrott, F.A., Perrott, R.A., Metzger, P., Eglinton, G., 1999. Glacial-interglacial environmental changes inferred from molecular and compound specific $\delta^{13}\text{C}$ analysis of sediments from Sacred Lake, Mt. Kenya. *Geochimica et Cosmochimica Acta* 63, 1383–1404.
- Huang, Y., Dupont, L., Sarnthein, M., Hayes, J.M., Eglinton, G. Mapping of C_4 plant input from North West Africa into North East Atlantic sediments. *Geochimica et Cosmochimica Acta*, submitted for publication.
- Ishiwatari, R., Hirakawa, Y., Uzaki, M., Yamada, K., Yada, T., 1994. Organic geochemistry of the Japan Sea sediments — I: bulk organic matter and hydrocarbon analyses of Core KH-79-3, C-3 from the Oki Ridge for paleoenvironment assessments. *Journal of Oceanography* 50, 179–195.
- Jordan, R.W., Zhao, M., Eglinton, G., Weaver, P.P.E., 1996. Coccolith and alkenone stratigraphy and palaeoceanography at an upwelling site off NW Africa (ODP 658C) during the last 130,000 years. In: Mogailevsky, A.L., Whately, R.C. (Eds.), *Microfossils and Oceanic Environments*. University of Wales Press, Aberystwyth, pp. 111–130.
- Joussau, S. and 35 co-authors, 1999. Monsoon changes for 6000 years ago: results of 18 simulations from the Paleoclimate Modeling Intercomparison Project (PMIP). *Geophysical Research Letters* 26, 859–862.
- Jouzel, J., Lorius, C., Petit, J.R., Genthon, C., Barkov, N.I., Kotlyakov, V.M. et al., 1987. Vostoc Ice core: a continuous isotope temperature record over the last climatic cycle (160,000 years). *Nature* 329, 403–408.
- Leuenberger, M., Siegenthaler, U., Langway, C.C., 1992. Carbon isotope composition of atmospheric CO_2 during the last ice age from an Antarctic ice core. *Nature* 357, 488–490.
- Madureira, L.A.S., van Kreveld, S.A., Eglinton, G., Conte, M.H., Ganssen, G., van Hinte, J.E. et al., 1997. Late Quaternary high-resolution biomarker and other sedimentary climate proxies in a northeast Atlantic core. *Paleoceanography* 12, 255–269.
- Maslin, M., Sarnthein, M., Knaack, J.-J., 1996. Subtropical Eastern Atlantic climate during the Eemian. *Naturwissenschaften* 83, 122–126.

- Mix, A.C., Ruddiman, W.F., McIntyre, A., 1986. Late Quaternary paleoceanography of the tropical Atlantic, 1: Spatial variability of annual mean sea-surface temperature, 0–20,000 years B. P. *Paleoceanography* 1, 43–66.
- Molfini, B., McIntyre, A., 1990. Precessional forcing of nutrient dynamics in the Equatorial Atlantic. *Science* 249, 766–769.
- Müller, P.J., Suess, E., 1979. Productivity, sedimentation rate, and sedimentary organic carbon in the oceans — I. Organic carbon preservation. *Deep-Sea Research* 26, 1347–1362.
- Muller, P.J., Schneider, R., Ruhland, G., 1994. Late Quaternary P_{CO_2} variations in the Angola Current: Evidence from organic carbon $\delta^{13}\text{C}$ and alkenone temperatures. In: Zahn, R., Kaminski, M.A., Labeyrie, L., Pedersen, T.F. (Eds.), *Carbon Cycling in the Glacial Ocean: Constraints On The Ocean's Role In Global Change NATO ASI Series I*, vol.17., Springer, Berlin, pp. 343–366.
- Nigrini, C., Caulet, J.-P., 1992. Late Neogene radiolarian assemblages characteristic of Indo-Pacific areas of upwelling. *Micropaleontology* 38, 139–164.
- Pelejero, C., Kienast, M., Wang, L., Grimalt, J., 1999. The flooding of Sundaland during the last deglaciation: imprints in hemipelagic sediments from the southern South China Sea. *Earth and Planetary Science Letters* 171, 661–671.
- Pokras, E.M., Mix, A.C., 1985. Eolian evidence for spatial variability of late Quaternary climates in tropical Africa. *Quaternary Research* 24, 137–149.
- Poynter, J.G., Farrimond, P., Robinson, N., Eglinton, G., 1989a. Aeolian-derived higher plant lipids in the marine sedimentary record: links with paleoclimate. In: Leinen, M., Sarnthein, M. (Eds.), *Paleoclimatology and Palometeorology: Modern And Past Patterns Of Global Atmospheric Transport. NATO ASI Series 282*. Kluwer, pp. 435–462.
- Poynter, J.G., Farrimond, P., Brassell, S.C., Eglinton, G., 1989b. Molecular stratigraphic study of sediments from Holes 658A and 660A, Leg 108. *Proceedings of the Ocean Drilling Program, Scientific Results* 108, 387–394.
- Prahl, F.G., Muehlhausen, L.A., Zahnle, D.L., 1988. Further evaluation of long-chain alkenones as indicators of paleoceanographic conditions. *Geochimica et Cosmochimica Acta* 52, 2303–2310.
- Pye, A.C., 1987. *Eolian Dust and Dust Deposits*. Academic Press, New York.
- Ruddiman, W.F., Sarnthein, M., Backman, J., Baldauf, J.G., Curry, W., Dupont, L.M. et al., 1989. Late Miocene to Pleistocene evolution of climate in Africa and the low-latitude Atlantic: overview of leg 108 results. *Proceedings of the Ocean Drilling Program, Scientific Results* 108, 463–484.
- Sarnthein, M., Tetzlaff, G., Koopmann, B., Wolter, K., Pflaumann, U., 1981. Glacial and interglacial wind regimes over the eastern subtropical Atlantic and North-West Africa. *Nature* 293, 193–196.
- Sarnthein, M., Thiede, J., Pflaumann, U., Erlenkeuser, H., Futterer, D., Koopmann, B. et al., 1982. Atmospheric and oceanic circulation patterns off Northwest Africa during the past 25 million years. In: von Rad, U., Hinz, K., Sarnthein, M., Seibold, E. (Eds.), *Geology of the Northwest African Continental Margin*. Springer-Verlag, Berlin, pp. 545–603.
- Sarnthein, M., Pflaumann, U., Ross, R., Tiedemann, R., Winn, K., 1992. Transfer functions to reconstruct ocean palaeoproductivity: a comparison. In: Summerhayes, C.P., Prell, W.L., Emeis, K.C. (Eds.), *Upwelling Systems: Evolution since the Early Miocene*. Geological Society Special Publication No. 64., The Geological Society, London, pp. 411–427.
- Schneider, R., Müller, P.J., Ruhland, G., 1995. Late Quaternary surface circulation in the east equatorial South Atlantic: evidence from alkenone sea surface temperature. *Paleoceanography* 10, 197–219.
- Simoneit, B.R.T., 1997. Compound-specific carbon isotope analyses of individual long-chain alkanes and alkanolic acids in Harmattan aerosols. *Atmospheric Environment* 31, 2225–2233.
- Simoneit, B.R.T., Chester, R., Eglinton, G., 1977. Biogenic lipids in particulates from the lower atmosphere over the eastern Atlantic. *Nature* 267, 682–685.
- Street-Perrott, F.A., Huang, Y., Perrott, R.A., Eglinton, G., Barker, P., Khelifa, L.B. et al., 1997. Impact of lower atmospheric carbon dioxide on tropical mountain ecosystems. *Science* 278, 1422–1426.
- Tetzlaff, G., Wolter, W., 1980. Meteorological patterns and the transport of mineral dust from the north African continent. *Paleoecology of Africa* 12, 31–42.
- Tiedemann, R., 1991. Acht Millionen Jahre Klimageschichte von Nordwest Afrika und Paläozoographie des angrenzenden Atlantiks: Hochauflösende Zeitreihen von ODP Sites 658–661. PhD thesis, University of Kiel, Kiel, Germany.
- Van de Water, P.K., Leavitt, S.W., Betancourt, J.L., 1994. Trends in stomatal density and $^{13}\text{C}/^{12}\text{C}$ ratios of *Pinus flexilis* needles during last glacial–interglacial cycle. *Science* 264, 239–243.
- Venec-Peyre, M.T., Caulet, J.P., Vergnaud-Grazzini, C., 1995. Paleohydrographic changes in the Somali Basin (5°N upwelling and equatorial areas) during the last 160 kyr, based on correspondence analysis of foraminiferal and radiolarian assemblages. *Paleoceanography* 10, 473–491.
- Vergnaud-Grazzini, C., Venec-Peyre, M.T., Caulet, J.P., Lerasle, N., 1995. Fertility tracers and monsoon forcing at an equatorial site of the Somali Basin (northwest Indian Ocean). *Marine Micropaleontology* 26, 137–152.
- Westerhausen, L., Poynter, J., Eglinton, G., Erlenkeuser, H., Sarnthein, M., 1993. Marine and terrigenous origin of organic matter in modern sediments of the equatorial East Atlantic: the $\delta^{13}\text{C}$ and molecular record. *Deep-Sea Research* 40, 1087–1121.
- Winn, K., Sarnthein, M., Erlenkeuser, H., 1991. $\delta^{18}\text{O}$ stratigraphy and chronology of Kiel sediment cores from the East Atlantic. Report no. 45. Geologisch-Paläontologisches Institut, Universität Kiel, pp. 1–100.
- Yamada, K., Ishiwatari, R., 1999. Carbon isotopic compositions of long-chain n-alkanes in the Japan Sea sediments: implications for paleoenvironmental change over the past 85kyr. *Organic Geochemistry* 30, 367–377.
- Zhao, M., Rosell, A., Eglinton, G., 1993. Comparison of two U_{37}^K sea surface temperature records for the last climatic cycle at ODP site 658 from the sub-tropical Northeast Atlantic. *Paleoceanography, Palaeoclimatology and Palaeoecology* 103, 57–65.
- Zhao, M., Beveridge, N.A.S., Shackleton, N.J., Sarnthein, M., Eglinton, G., 1995. Molecular stratigraphy of cores off Northwest Africa: sea surface temperature history over the last 80 ka. *Paleoceanography* 10, 661–675.